



Stresses in finite anisotropic plate weakened by rectangular hole



Mihir M Chauhan^a, Dharmendra S Sharma^{b,*}

^a Institute of Technology, Nirma University, Ahmedabad 382481, Gujarat, India

^b Faculty of Technology and Engineering, The M S University of Baroda, Vadodara 390002, Gujarat, India

ARTICLE INFO

Article history:

Received 6 May 2015

Received in revised form

20 July 2015

Accepted 5 August 2015

Available online 12 August 2015

Keywords:

Boundary collocation

Complex variable method

Finite plate

Rectangular hole

Stress concentration

ABSTRACT

In this paper, a solution to calculate the stress components around rectangular shaped cutout in a finite anisotropic plate subjected to in-plane loading is presented. The stress functions are derived using complex variable approach and least square boundary collocation method. The influence of plate size, material properties, stacking sequence, hole geometry and loading conditions on the stress concentration is also presented. Some of the results obtained by present method are compared with finite element solutions and with the existing literature.

© 2015 Elsevier Ltd. All rights reserved.

1. Introduction

Thin plates of various materials are very commonly used in engineering applications. The different shapes of cutouts are made in plates to cater the need of service/operation. These cutouts exhibit high stress concentration under different loading condition and may cause the catastrophic failure of the components. To understand the catastrophe of the component, it is necessary to have an awareness of the stress concentration around the hole in a plate during design phase.

The closed form solutions for the stresses around different shaped holes in an infinite isotropic and anisotropic plate for different loading have been obtained by Savin [1], Lekhnitskii [2], Ukadgaonker and Rao [3], Rao et al. [4], Sharma [5–7], Sharma et al. [8], Sharma and Dave [9], Patel and Sharma [10], Rezaeepazhand and Jafari [11], Batista [12], Yang et al. [13] and many more using complex variable approach proposed by Muskhelishvili [14]. In all these solutions the load is assumed to be applied at the remote boundary of the plate (i.e. infinite plate) which is not always the case in practical applications like perforated plates, aircrafts windows, automobile windows etc. wherein the loaded boundaries are nearer to the hole and affect the stress distribution around the hole severely. The cases where the boundary are closer to the hole or other way if the ratio of the plate size to the hole size

is less than 10, it is considered as the finite plate. The stress distribution around hole in finite plate cannot be estimated through the solution of infinite plate directly.

Some researchers namely Ogonowski [15], Newman [16], Lin and Ko [17], Woo and Chan [18], Madenci et al. [19], Xiwu et al. [20], Xu et al. [21], Zheng and Xu [22] and few others have proposed the solutions for finite plate using complex variable method. The complex stress functions are expressed in terms of infinite power series and the constants of the series are obtained by boundary collocation method. These solutions are limited to circular and/or elliptical hole in isotropic and/or anisotropic finite plate. In many engineering applications the shape of the hole is not only limited to circular or elliptical but the rectangular and polygonal holes are also found its practical importance. The solution for stresses around rectangular hole in finite plate is proposed by Pan et al. [23] by modified stress functions for isotropic material. The literature review suggests that the solution for the stresses around rectangular and square shaped hole in finite laminated plate has not been addressed.

The present work provides a generalized method to obtain the stress distribution around rectangular hole in finite anisotropic plate. Unlike the previous papers, a generalized Schwarz–Christoffel mapping function is used in the formulation of anisotropic finite plate to map the rectangular hole on to the unit circular hole. The Laurent series expansion of the complex stress functions is used and constants of the series are derived using the boundary collocation method. Influence of plate size, hole geometry, material properties and stacking sequence on stress concentration are also studied and presented.

* Corresponding author. Mobile: +91 9879472897.

E-mail addresses: mihir.chauhan@gmail.com (M. Chauhan), dss_iit@yahoo.com (D. Sharma).

2. Analytical formulation

A finite sized thin plate having rectangular opening (refer Fig. 1) is subjected to in-plane loading. Applying generalized Hooke's law, Airy's stress functions and strain–displacement compatibility conditions, the stress components in an anisotropic media can be represented in terms of Muskhelishvili's [14] complex stress functions $\phi_j(z_j)$ as

$$\begin{aligned} \sigma_x &= 2\text{Re} \left[\sum_{j=1}^2 \mu_j^2 \phi_j'(z_j) \right] \\ \sigma_y &= 2\text{Re} \left[\sum_{j=1}^2 \phi_j'(z_j) \right] \\ \tau_{xy} &= 2\text{Re} \left[\sum_{j=1}^2 \mu_j \phi_j'(z_j) \right] \end{aligned} \quad (1)$$

where, $z_j = x + \mu_j y$, μ_j are the complex constants of anisotropy. These constants are roots of the characteristics equation of anisotropic plate (Lekhnitskii [2]) and depend on material properties, fiber orientation and stacking sequence.

2.1. Mapping function

The mapping function to map the area external to the rectangular shaped cutout in z -plane conformally on to the area outside the unit circle in ζ - plane is available in the literature [1] as follows:

$$z = R \left(\zeta + \sum_k \frac{C_k}{\zeta^k} \right) \quad (k = 2p - 1, p = 1, 2, 3, \dots, n) \quad (2)$$

where R is the size factor, $\zeta = e^{i\theta}$ and C_k are the constants of the mapping functions. The values of constants of mapping functions are available in the literature for few specific side ratios of rectangle having longer side parallel to X -axis. To produce the rectangle of any desired side ratios (D/d) and also at any orientations (α), the constants of the mapping functions (C_k) are obtained as follows:

$$\begin{aligned} C_1 &= \frac{1}{2} \left(e^{2i(\beta+\alpha)} + e^{-2i(\beta-\alpha)} \right); \\ C_3 &= \frac{1}{24} \left(e^{2i(\beta+\alpha)} - e^{-2i(\beta-\alpha)} \right)^2; \\ C_5 &= \frac{1}{80} \left(e^{4i(\beta+\alpha)} - e^{-4i(\beta-\alpha)} \right) \left(e^{2i(\beta+\alpha)} - e^{-2i(\beta-\alpha)} \right); \end{aligned} \quad (3)$$

where β characterizes the side ratio of the rectangular hole (refer Table 1) and α is orientation angle of rectangular hole with positive X axis as shown in Fig. 1. Table 1 shows the values of these constants for different side ratios of rectangular hole with the corner radius (ρ) and total perimeter. The corner radius is derived using the formula given by Sharma [5].

For an anisotropic media, Eq. (2) is modified by introducing constants of anisotropy μ_j . Due to affine transformation, Eq. (2) takes the form

$$z_j = R \left[a_j \left(\frac{1}{\zeta} + \sum_k C_k \zeta^k \right) + b_j \left(\zeta + \sum_k \frac{C_k}{\zeta^k} \right) \right] \quad (4)$$

where, $a_j = (1 + i\mu_j)/2$, $b_j = (1 - i\mu_j)/2$ and C_k are the constants corresponding to the different side ratios of the rectangular hole.

Rearranging the terms in Eq. (4), a polynomial equation of ζ is obtained as

$$\sum_k \left[Ra_j C_k \zeta^{2k} + Rb_j \zeta^{k+1} - z_j \zeta^k + a_j \zeta^{k-1} + b_j C_k \right] = 0 \quad (5)$$

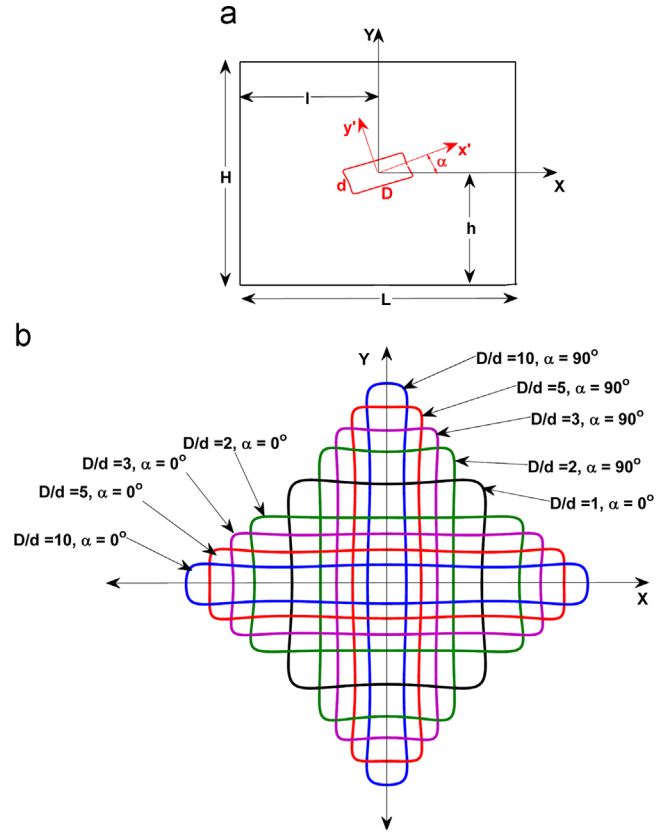


Fig. 1. Geometry of finite plate and rectangular hole.

Table 1
Constants of mapping functions.

D/d $\alpha = 0$	β	C_1	C_3	C_5	Corner radius (ρ)	Total perimeter
1	0.7983	-0.0251	-0.1666	0.0025	0.0996	6.68
2	0.6283	0.3095	-0.1507	-0.0280	0.0679	6.79
3	0.5364	0.4781	-0.1286	-0.0369	0.0548	6.93
4	0.4764	0.5797	-0.1107	-0.0385	0.0554	7.03
5	0.4333	0.6477	-0.0967	-0.0376	0.0597	7.10
6	0.4003	0.6965	-0.0858	-0.0359	0.0649	7.16
7	0.3741	0.7331	-0.0771	-0.0339	0.0710	7.22
8	0.3525	0.7617	-0.0700	-0.0320	0.0761	7.26
9	0.3345	0.7847	-0.0640	-0.0302	0.0808	7.30
10	0.3190	0.8035	-0.0591	-0.0285	0.0848	7.34

The one out of $2k$ roots of Eq. (5) maps the rectangle shape on to the unit circle and it is used for the solution of stress function.

2.2. Stress functions

The stress functions can be taken in the form of infinite power series with negative and positive power terms in ζ_j plane as [2],

$$\varphi_j(\zeta_j) = \alpha_j \ln \zeta_j + \sum_{m=1}^{\infty} \left(A_{jm} \zeta_j^{-m} + B_{jm} \zeta_j^m \right), \quad (6)$$

where, α_j , A_{jm} and B_{jm} are unknown constants of the series which are derived from boundary conditions, ζ_j are the mapped

coordinates obtained from Eq. (5) corresponding to z_j . In Eq. (6) the positive power terms define analytic function on the plate boundary while the negative power terms along with the logarithmic terms define analytic function on the hole boundary. For the traction free condition of the hole, the logarithmic terms are dropped.

2.3. Boundary conditions

Forces acting on the boundary of the plate in X and Y direction can be written in terms of complex stress functions as [19]

$$\pm F_x = 2\text{Re} \sum_{j=1}^2 \mu_j (\phi_j(\zeta_j) - \phi_j(\zeta_j^0)),$$

$$\mp F_y = 2\text{Re} \sum_{j=1}^2 (\phi_j(\zeta_j) - \phi_j(\zeta_j^0)), \tag{7}$$

where, ζ_j^0 is the mapped coordinate of the reference point on the boundary. Substituting Eq. (6) in to Eq. (7) and rearranging the terms

$$\pm F_x = 2\text{Re} \left[\sum_{m=1}^{\infty} \sum_{j=1}^2 \mu_j [(\zeta_j^{-m} - \zeta_j^{0-m})A_{jm} + (\zeta_j^m - \zeta_j^{0m})B_{jm}] \right],$$

$$\mp F_y = 2\text{Re} \left[\sum_{m=1}^{\infty} \sum_{j=1}^2 [(\zeta_j^{-m} - \zeta_j^{0-m})A_{jm} + (\zeta_j^m - \zeta_j^{0m})B_{jm}] \right]. \tag{8}$$

The left hand side of Eq. (8) are the applied force on plate boundary. F_x and F_y can be written as $F_x = s_x(y - y_0)$, $F_y = s_y(x - x_0)$, where, x and y are the coordinates of respective collocation points while x_0 and y_0 are coordinates of reference point on the boundary, s_x and s_y can be set as follows [4]:

$$s_x = \frac{\sigma}{2} [(\lambda + 1) - \text{Re}((\lambda - 1)e^{2i\gamma})],$$

$$s_y = \frac{\sigma}{2} [(\lambda + 1) + \text{Re}((\lambda - 1)e^{2i\gamma})], \tag{9}$$

where σ is applied loading on the plate boundary, λ is the loading factor which can be set to 0 or 1 for uniaxial or equi-biaxial loading respectively and γ is load angle with respect to positive X axis.

3. Solution methodology

To obtain the stress components in the finite plate with rectangular hole, N_1 number of collocation points on plate boundary and N_2 numbers of collocation points on the hole boundary are generated in z-plane. Each collocation point of z-plane is mapped to the respective point in ζ - plane by using mapping function (Eq. (5)). Imposing the boundary conditions (Eq. (8)) on each collocation point $2N$ ($N = N_1 + N_2$) number of boundary equations are generated. These equations are solved simultaneously to determine the constants of the series. If the series in stress functions are

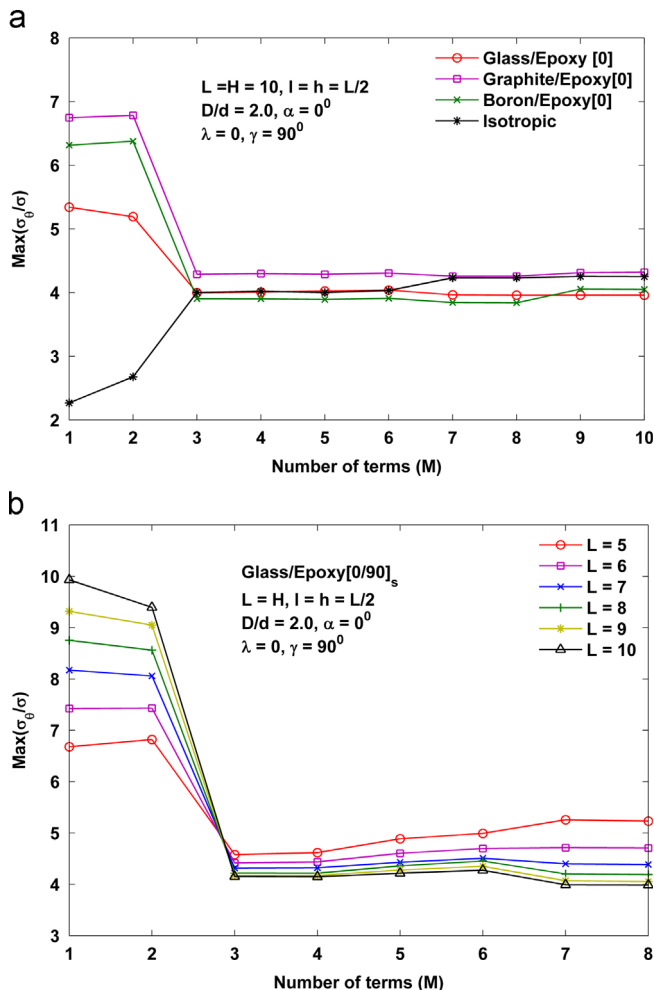


Fig. 2. Convergence of the results.

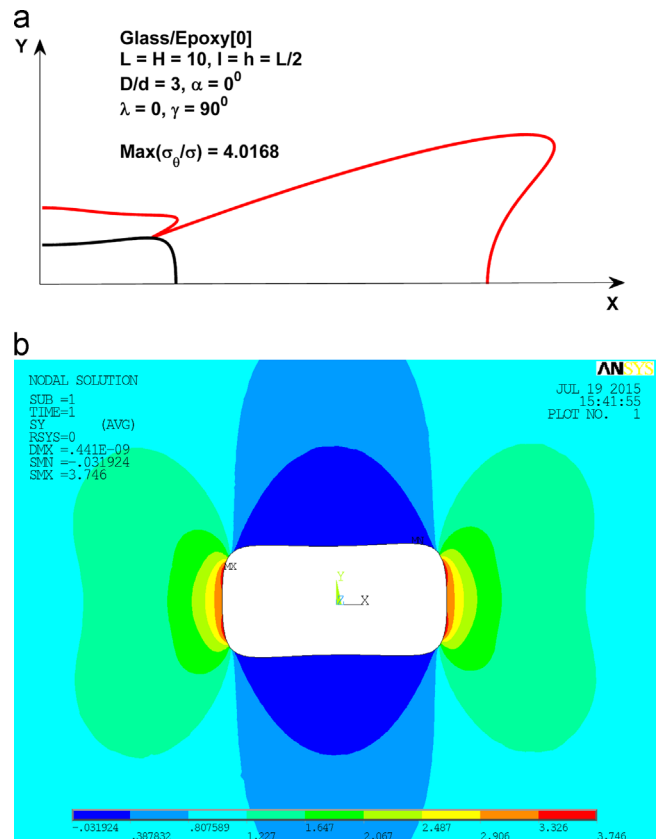


Fig. 3. Stress distribution around rectangular hole (a) Present method, (b) ANSYS.

truncated to a finite number M , total $4M$ number of unknowns are to be determined from $2N$ number of boundary equations.

The need of large number of collocation points to define the boundaries accurately results in overdetermined system of equations i.e. $2N \gg 4M$. This overdetermined system of Eq. ((10)) is solved using the least square method.

$$[P]_{(2N \times 4M)} [X]_{(4M \times 1)} = [F]_{(2N \times 1)}, \tag{10}$$

where $[P]$ is the matrix of coefficients, $[X]$ is the vector of unknowns and $[F]$ is the known vector of boundary force.

An iterative process of increasing the number of terms in series up to some finite number is employed till the convergence is achieved. Once the constants of the series stress functions are known, the stress components can be evaluated using Eq. (1). The stresses in the polar coordinate are determined using stress transformation.

4. Results and discussion

The mathematical formulation and solution methodology is presented in the previous section. Based on the formulation, a computer program is prepared to obtain the stress distribution around rectangular hole in a finite anisotropic plate. The loading parameters (σ, λ and γ), material properties (E_1, E_2, G_{12} and ν_{12}), stacking sequence, plate size (L and H) and hole geometry (n, β, α) are input to the program. Fig. 1(a) shows the geometry of finite plate with rectangular hole and Fig. 1(b) shows the hole with different side ratios and orientations. For 0° orientation, the longer side (D) of the rectangle is parallel to X axis while it is parallel to Y axis for 90° orientation. The materials considered here are Graphite/Epoxy ($E_1 = 182$ GPa, $E_2 = 10.3$ GPa, $G_{12} = 7.17$ GPa, $\nu_{12} = 0.28$), Glass/Epoxy ($E_1 = 47.4$ GPa, $E_2 = 16.2$ GPa, $G_{12} = 7$ GPa, $\nu_{12} = 0.26$), Plywood ($E_1 = 11.79$ GPa, $E_2 = 5.89$ GPa, $G_{12} = 0.69$ GPa, $\nu_{12} = 0.071$), Boron/Epoxy ($E_1 = 282.77$ GPa, $E_2 = 23.79$ GPa, $G_{12} = 10.35$ GPa, $\nu_{12} = 0.27$) and Isotropic steel ($E = 205$ GPa, $G = 80$ GPa, $\nu = 0.26$).

The representation of the stress functions in terms of infinite power series needs the checking of convergence to produce accurate results. The convergence of series is affected by number of collocation points, plate size, hole geometry and material properties. To check the convergence of the series, an iterative process of increasing the number of terms in the series stress functions is employed and the stress concentration around the hole is evaluated for each iteration. Fig. 2(a) shows the convergence of the stress concentration around rectangular hole with $D/d = 2$ in the finite ($L = H = 10$) plate of Glass/Epoxy[0], Graphite/Epoxy[0], Boron/Epoxy[0] and isotropic material subjected to uniaxial Y loading. The convergence for the different plate size is shown in Fig. 2(b) for Glass/Epoxy[0/90]_s laminated plate subjected to uniaxial Y loading. Fig. 2(c) shows the convergence of results in the laminated plate of size $L = H = 10$ subjected to uniaxial load. The good convergence of the results is achieved.

To validate the results obtained through present method, a comparison with the finite element solution (ANSYS) is shown in Fig. 3 and Fig. 4. The maximum normalized stress around the rectangular hole ($D/d = 3.0$) in finite ($L = H = 10$) Glass/Epoxy [0] plate is 4.016 and 3.746 respectively through the present method (Fig. 3(a)) and ANSYS (Fig. 3(b)) for uniaxial tensile load. The maximum normalized stress around the square hole ($D/d = 1.0$) in finite ($L = H = 10$) isotropic plate is 4.149 and 4.237 respectively through the present method (Fig. 4(a)) and ANSYS (Fig. 4(b)) for uniaxial tensile load. In Finite element model PLANE182 and PLANE42 elements are used for orthotropic plate and isotropic plate, respectively. The exact geometry of the plate with hole is

produced in ANSYS by exporting the coordinates of key-points through a computer program. The results obtained through present method are in close agreement with that of the finite element solutions.

The stress concentration around rectangular hole of different side ratios are obtained for the finite plate of Glass/Epoxy[0], Glass/Epoxy[90], Glass/Epoxy[0/90]_s, Graphite/Epoxy[0/90]_s and Graphite/Epoxy[0₄/±45/90₂]_s subjected to uniaxial load as shown in Table 2. It is observed from Table 2 that for a given plate size, the stress concentration increases as the side ratio increases (for $D/d \geq 1$). The increase in side ratio produces the narrow and elongated rectangle that raises the stress concentration. Additionally, the narrow and elongated rectangular hole has vertices closer to the plate boundary that makes the stress concentration more severe.

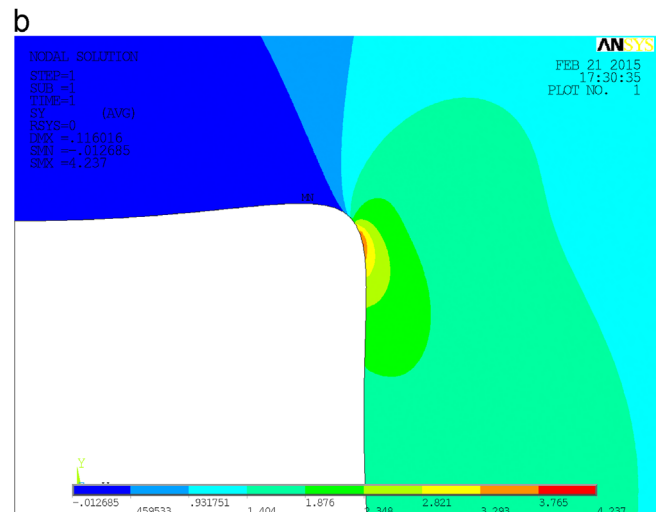
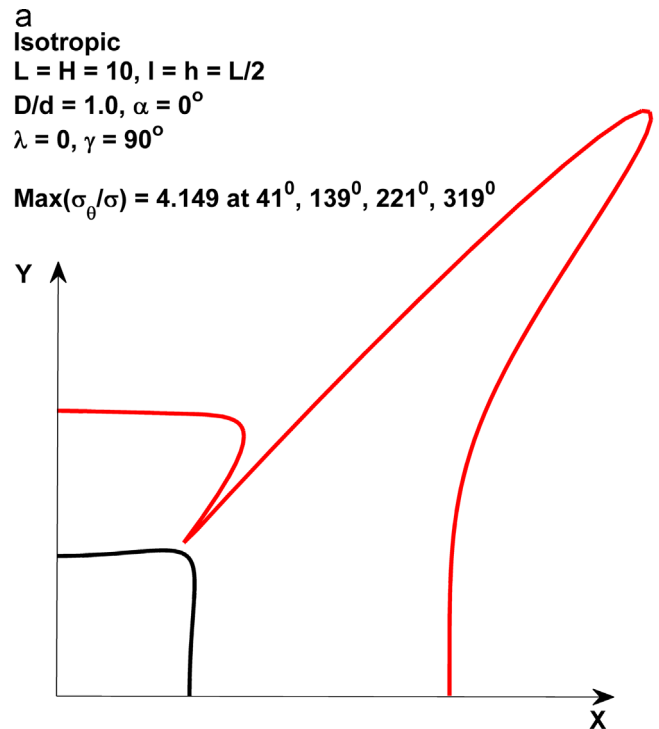


Fig. 4. Stress distribution around square hole (a) Present method, (b) ANSYS.

Table 2
 Max(σ_{θ}/σ) around centrally located rectangular hole in square plate ($L=H$).

L	D/d									
	1	2	3	4	5	6	7	8	9	10
Glass/Epoxy [0] $\lambda=0, \gamma=90^\circ, \alpha=0^\circ$										
5	4.24	4.78	5.13	5.60	6.51	7.94	9.02	10.47	11.68	12.73
6	3.96	4.40	4.66	5.52	5.96	7.01	8.04	9.59	10.30	11.37
7	3.84	4.19	4.35	4.72	5.48	6.60	7.61	8.71	9.69	10.56
8	3.76	4.06	4.19	4.52	5.21	6.18	7.09	8.12	9.30	10.13
9	3.71	4.00	4.08	4.38	5.07	5.92	6.84	7.87	8.99	9.77
10	3.69	3.96	4.02	4.28	4.90	5.74	6.88	7.61	8.51	9.57
100	3.59	3.86	3.97	4.24	4.78	5.59	6.41	7.23	8.03	8.86
Infinite	3.83	3.91	4.03	4.28	4.85	5.66	6.48	7.30	8.11	8.91
Glass/Epoxy [90] $\lambda=0, \gamma=90^\circ, \alpha=0^\circ$										
6	4.72	6.31	7.23	9.02	11.38	13.70	16.18	18.70	21.30	23.86
8	4.52	5.82	6.61	8.34	9.93	11.53	13.47	15.31	17.35	19.22
10	4.33	6.04	6.76	8.15	9.49	11.17	12.79	14.38	15.86	17.51
100	3.79	4.41	4.93	6.09	7.50	8.90	10.30	11.70	13.08	14.46
Infinite	4.82	4.82	5.06	6.16	7.57	8.97	10.38	11.76	13.15	14.53
Glass/Epoxy [0/90] _s $\lambda=0, \gamma=90^\circ, \alpha=0^\circ$										
6	4.31	5.22	5.66	6.79	7.59	8.32	9.95	11.61	13.23	14.88
8	4.01	4.93	5.38	6.22	7.21	7.59	9.05	10.22	11.73	12.96
10	3.79	4.78	5.20	5.96	6.23	8.60	9.71	11.12	12.26	13.44
100	3.54	4.02	4.34	5.09	6.31	7.37	8.51	9.63	10.75	11.86
Infinite	3.51	4.02	4.40	5.17	6.31	7.44	8.57	9.69	10.81	11.93

Table 3
Max (σ_{θ}/σ) around rectangular hole in square plate ($L=10$).

D/d	α	Glass/Epoxy [0/90] _s			Glass/Epoxy [0 ₄ /±45/90 ₂] _s			Glass/Epoxy [0]			Isotropic		
		$\lambda=0, \gamma=0^\circ$	$\lambda=0, \gamma=90^\circ$	$\lambda=1, \gamma=0^\circ$	$\lambda=0, \gamma=0^\circ$	$\lambda=0, \gamma=90^\circ$	$\lambda=1, \gamma=0^\circ$	$\lambda=0, \gamma=0^\circ$	$\lambda=0, \gamma=90^\circ$	$\lambda=1, \gamma=0^\circ$	$\lambda=0, \gamma=0^\circ$	$\lambda=0, \gamma=90^\circ$	$\lambda=1, \gamma=0^\circ$
1	0°	4.09	3.79	5.28	3.76	3.72	5.66	4.23	3.69	5.95	3.84	3.84	6.21
2	0°	2.69	4.78	4.96	2.75	4.18	5.12	2.95	3.98	5.02	2.82	4.25	5.60
3	0°	2.03	5.20	4.80	2.03	4.43	4.66	2.16	4.02	4.40	2.12	4.47	5.03
4	0°	1.63	5.96	5.02	1.63	4.87	4.58	1.73	4.29	4.20	1.69	4.88	4.85
5	0°	1.35	7.21	6.08	1.36	5.77	4.96	1.48	4.91	4.43	1.40	5.59	5.02
6	0°	1.16	8.60	7.47	1.17	6.82	5.90	1.28	5.74	5.09	1.20	6.62	5.62
7	0°	1.11	9.71	8.60	1.06	7.86	6.94	1.20	6.88	6.20	1.05	7.68	6.64
8	0°	1.12	11.12	10.00	1.05	8.93	8.01	1.14	7.61	6.96	1.05	8.73	7.69
9	0°	1.11	12.26	11.15	1.05	9.95	9.02	1.13	8.50	7.86	1.05	9.79	8.74
10	0°	1.10	13.44	12.34	1.04	11.07	10.15	1.14	9.56	8.90	1.05	10.84	9.79
10	90°	13.42	1.10	12.32	12.80	1.22	11.58	17.44	1.88	15.56	10.97	1.08	9.90
9	90°	12.14	1.11	11.03	11.55	1.21	10.34	15.83	1.88	13.95	9.90	1.07	8.83
8	90°	10.92	1.11	9.81	10.30	1.21	9.10	14.19	1.87	12.31	8.83	1.07	7.77
7	90°	9.65	1.12	8.53	9.07	1.20	7.86	12.57	1.86	10.71	7.76	1.06	6.70
6	90°	8.41	1.17	7.29	7.83	1.20	6.63	10.99	1.85	9.14	6.69	1.20	5.66
5	90°	7.28	1.36	6.15	6.60	1.36	5.43	9.43	1.84	7.59	5.64	1.40	5.04
4	90°	6.06	1.62	5.15	5.47	1.63	4.85	7.86	1.82	6.12	4.91	1.69	4.86
3	90°	5.34	2.02	4.91	4.80	2.04	4.84	6.58	2.08	5.66	4.49	2.12	5.03
2	90°	4.70	2.77	4.87	4.39	2.73	5.20	5.98	2.75	5.93	4.26	2.83	5.61
1	90°	3.97	3.82	5.27	3.76	3.72	5.66	4.23	3.68	5.93	3.84	3.84	6.21

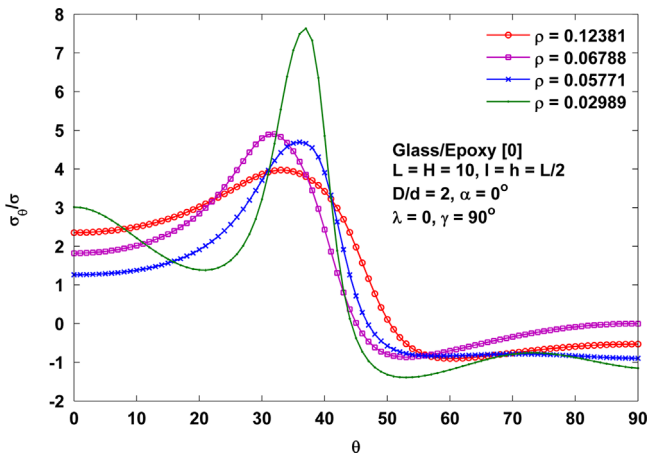


Fig. 6. Effect of corner radius (ρ)

Table 4
Effect of hole orientation angle (α) on Max(σ_{θ}/σ) ($\lambda=0, \gamma=0^\circ, L=H=10, l=h=L/2, D/d=1$)

α	Isotropic	Glass/Epoxy[0]	Glass/Epoxy[90]	Glass/epoxy[0/90] _s
0°	3.84	4.23	3.80	4.09
5°	2.30	9.62	4.90	7.19
10°	2.92	15.80	7.60	10.14
15°	3.02	18.44	10.85	12.85
20°	2.69	20.83	6.68	15.23
25°	3.29	22.77	16.94	17.37
30°	4.87	21.57	10.89	19.88
35°	5.88	16.80	9.54	21.81
40°	4.79	16.34	8.54	23.10
45°	8.91	13.49	7.61	23.70
50°	4.95	16.51	8.36	23.59
55°	6.06	16.99	9.39	22.79
60°	5.09	21.87	10.89	21.32
65°	3.40	22.89	17.06	19.22
70°	2.77	19.20	5.82	16.55
75°	3.38	18.38	9.33	13.39
80°	2.99	15.11	7.19	9.85
85°	2.36	9.86	4.72	6.03
90°	3.84	4.23	3.94	3.79

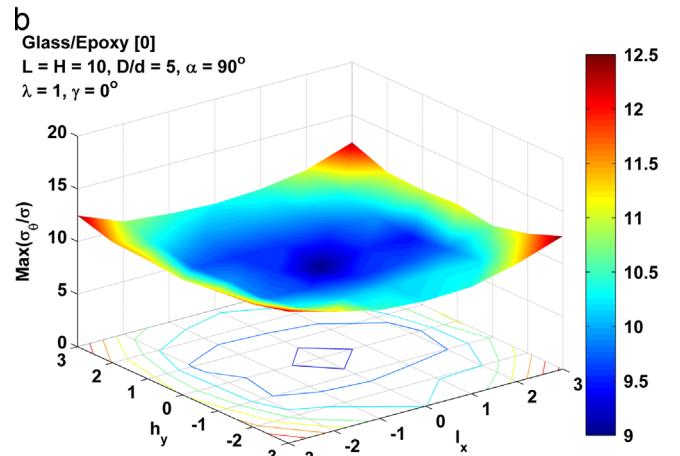
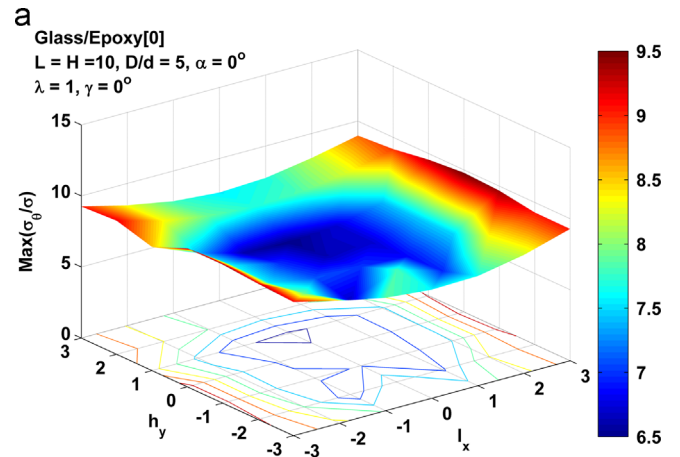


Fig. 7. Effect of hole location.

plate. To study this effect, the vertex location is altered by two different ways, (a) by changing the orientation of the hole about its center i.e. by varying α and (b) by changing the location of hole center keeping orientation constant i.e. by varying l and h .

Table 4 shows the effect of α (for case (a)) on stress concentration around square hole ($D/d=1$) in finite plate ($L=H=10$) subjected to uniaxial load. The maximum stress concentration for isotropic plate and Glass/Epoxy[0/90]_s is observed at 45° rotation while for Glass/Epoxy[0] and Glass/Epoxy[90] plate, the maximum stress concentration is observed at 25° and 65°.

For case (b), to change the location of the hole with respect to plate boundary, the x and y coordinates of hole center with respect to the center of plate are defined as $l_x = l - (L/2)$ and $h_y = h - (H/2)$ respectively and are varied (by varying l and h) to obtain various positions of the hole in a finite plate. For each hole location in Glass/Epoxy [0] plate, maximum normalized stress is derived and a surface plot is obtained for $D/d=5$ with 0° and 90° orientation as shown in Fig. 7(a) and (b) respectively. The stress concentration is higher when the vertices of the rectangular hole is near to the plate boundary. Similar to this a family of contours for different geometry of plate and hole can be obtained for the use of estimating the stress concentration.

5. Conclusions

A generalized methodology is presented to obtain the stress functions for finite composite plate with rectangular hole using complex variable approach in conjunction with the boundary collocation method. The solution can be used as ready reference to the designers for estimating the stress concentration around the rectangular hole. The solution is also useful to predict the effect of material properties, stacking sequence, hole geometry, plate size and loading conditions on the stress distribution around rectangular hole. The method is capable to produce the satisfactory solution for infinite plate by considering the large plate size. The solution of isotropic plate can also be obtained by considering suitable material properties. By changing the constants of mapping function, the solution can be applied to other shapes of cutouts also.

References

- [1] Savin GN. Stress concentration around holes. New York: Pergamon Press; 1971.
- [2] Lekhnitskii SG. Anisotropic plates. New York: Gordon and Breach Science Publisher; 1968.
- [3] Ukadgaonker VG, Rao. DKN. A general solution for stress distribution around holes in symmetric laminates under in-plane loading. Compos Struct 2000;49:339–54.
- [4] Rao DKN, Babu MR, Reddy KRN, Sunil D. Stress around square and rectangular cutouts in symmetric laminates. Compos Struct 2010;92(12):2845–59.
- [5] Sharma DS. Stress distribution around polygonal holes. Int J Mech Sci 2012;65:115–24.
- [6] Sharma DS. Moment distribution around polygonal holes in infinite plate. Int J Mech Sci 2014;78:177–82.
- [7] Sharma DS. Stresses around polygonal hole in an infinite laminated composite plate. Eur J Mech A/Solids 2015;54:44–52.
- [8] Sharma DS, Patel NP, Trivedi RR. Optimum design of laminates containing an elliptical hole. Int J Mech Sci 2014;85:76–87.
- [9] Sharma DS, Dave JM. Stress intensity factors for hypocycloidal hole with cusp in infinite anisotropic plate. Theor Appl Fract Mech 2015;75:44–52.
- [10] Patel NP, Sharma DS. Bending of composite plate weakened by square hole. Int J Mech Sci 2015;94–95:131–9.
- [11] Rezaeepazhand J, Jafari M. Stress concentration in metallic plates with special shaped cutout. Int J Mech Sci 2010;52:96–102.
- [12] Batista M. On the stress concentration around a hole in an infinite plate subject to a uniform load at infinity. Int J Mech Sci 2011;53:254–61.
- [13] Yang Y, Liu J, Cai C. Analytical solutions to stress concentration problem in plates containing rectangular hole under biaxial tensions. Acta Mech Solida Sin 2008;21:411–9.
- [14] Muskhelishvili NI. Some Basic Problem of Mathematical Theory of Elasticity. The Netherland: P Noordhoff Ltd; 1962.
- [15] Ogonowski JM. Analytical study of finite geometry plates with stress concentrations. In: Proceedings of the AIAA/ASME/ASCE/AHS 21st SDM conference, Washington; 1980.
- [16] Newman JC. An improved method of collocation for the stress analysis of cracked plates with various shaped boundaries. Technical Note no. D-6376, NASA; 1971.
- [17] Lin CC, Ko CC. Stress and strength analysis of finite composite laminate with elliptical hole. J Comput Mat 1988;22:373–85.
- [18] Woo CW, LWS Chan. Boundary collocation method for analyzing perforated plate problem. Eng Fract Mech 1992;43(5):757–68.
- [19] Madenci E, Ileri L, Kudva JN. Analysis of finite composite laminates with holes. Int J Solids Struct 1993;30(6):825–34.
- [20] Xiwu XW, Liangxin S, Xuqi F. Stress analysis of finite composite laminates weakened by multiple elliptical holes. Int J Solids Struct 1995;32(20):3001–14.
- [21] Xu XW, Yue TM, Man HC. Stress analysis of finite composite laminate with multiple loaded holes. Int J Solids Struct 1999;36:919–31.
- [22] Zheng X, Xu X. Stress analysis of finite composite laminates with elliptical inclusion. Comput Struct 1999;70:357–61.
- [23] Pan Z, Cheng Y, Liu J. Stress analysis of a finite plate with a rectangular hole subjected to uniaxial tension using modified stress functions. Int J Mech Sci 2013;75:265–77.